Polarized Positive Muons Probing Free Radicals: A Variant of Magnetic Resonance

E. Roduner

Physikalisch-Chemisches Institut der Universität Zürich, Winterthurerstraße 190, CH-8057 Zürich, Switzerland

1 Introduction

What is an elementary particle which is classified as *anti*-matter and constitutes the main component of our exposure to cosmic rays on Earth good for in chemistry? Its microsecond lifetime makes it too elusive to allow the production of bottles of new compounds. Nevertheless, as will be shown here, the exotic particle forms the nucleus of an atom which is chemically well behaved. It can be substituted for protons in molecules where it acts as a spy, radiating off information of interest to the chemist.

The positive muon (μ^+) is a particle with a mass of one-ninth the proton mass, with spin $\frac{1}{2}$ and an associated magnetic moment which is 3.18 times the proton moment, and a lifetime of 2.2 μs. Its availability in the form of energetic beams with a spin polarization close to 100% at the ports of suitable accelerators led to its successful application as a magnetic probe in matter.[1] The four major accelerator facilities which operate such beams are found at TRIUMF in Canada, at PSI in Switzerland, at RAL in England, and at KEK in Japan. The experimental technique has been dubbed μSR, which stands for Muon Spin Rotation (or Resonance, or Relaxation).

In various materials the thermalizing muon captures an electron and forms a hydrogen-like one-electron atom with the muon as a nucleus. It has been dubbed muonium (Mu $\equiv \mu^+e^-$). Since its ionization potential and its Bohr radius are within 0.5% the same as those of H it is in a chemical sense a light hydrogen isotope.[2,3] It reacts with unsaturated bonds by addition, as in:

leaving thereby the muon as a polarized spin label chemically bound in a free radical. In this way it has proven particularly useful for the investigation of structure, reaction kinetics, and reorientational dynamics of organic radicals.[4]

Given the fact that the chemical and magnetic properties of a positive muon are completely analogous to those of the proton it is evident that the behaviour of the two nuclei in a magnetic field is also analogous and that phenomena of magnetic resonance such as precession, free induction decay, and relaxation can be described in much the same way in both cases. Whereas this is true in principle there are important differences which should be kept in mind. The short lifetime of the muon puts a severe limit on the spectral resolution and has the consequence that it is not possible to distinguish between different diamagnetic muon-substituted molecules since chemical shifts or nuclear couplings are not resolved. The muon is implanted in the sample as a polarized species. There is therefore no need to first create spin coherence using a high frequency preparation pulse. The time resolution is thus significantly increased over that of more conventional techniques. Furthermore one has close to the full muon polarization at all temperatures, and it is independent of the Curie factor which normally imposes a fatal limit on the experimental signal-to-noise ratio. This makes the muon technique extremely sensitive so that it is possible – and in time resolved experiments required – to work with a concentration of a single muon in the sample at a time. The immediate advantage of such low concentrations in radical chemistry is the absence of bimolecular termination reactions, which has the consequence that the kinetics are always of first or pseudo-first order and that the signal of surface-adsorbed radicals is not depleted under conditions of high radical mobility.

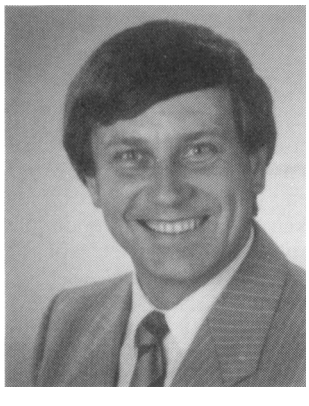

Emil Roduner is a physical chemist with interest in the formation, structure, and dynamics of organic free radicals in solid, liquid, and gaseous environments. In 1978 he made the first observation of muon-substituted free radicals. Since then he has been using positive muons as probes, and in 1988 he was awarded the Werner Prize and Medal for the development of the muon spin rotation technique to a universal method in radical chemistry.

$$\mu^+ \rightarrow e^+ + \nu_e + \tilde{\nu}_\mu \qquad (1)$$

Signal detection *via* energy absorption measurement is of course not feasible under conditions where one has a single muon in the sample, but fortunately, advantage can be taken of the asymmetric muon decay with emission of the decay positron preferentially in the instantaneous muon spin direction. On this basis, a single particle counting technique borrowed from particle physics allows monitoring a free induction decay signal in a *transverse* field experiment with a typical time resolution of *ca.* 1 ns, or to detect a time-integrated forward–backward decay asymmetry as a function of a *longitudinally* applied magnetic field.

The potential of the transverse field technique has been reviewed previously.[4] Emphasis will therefore be given here to the longitudinal field variant which takes advantage of the special effects encountered near avoided crossings of energy levels. They were first encountered in optical spectroscopy[5] but are used routinely in nuclear analytical methods[6] and in NMR, in particular together with fast field cycling methods.[7] They are also important for the mixing of radical pair singlet–triplet (S–T_{-1}) states in experiments studying electron polarization effects[8] and have found applications in many other areas of spectroscopy.[9] There are also other techniques which make use of nuclear spin polarized beams, which compared with NMR leads to an increased sensitivity in surface studies.[6]

2 Theoretical Background

2.1 Hamiltonian for a Radical with Axial Hyperfine Symmetry

In order to demonstrate the analogy of μSR with conventional magnetic resonance we concentrate on a system where the unpaired electron of a radical is coupled by hyperfine interaction to the muon and to one additional magnetic nucleus. Further magnetic nuclei introduce no major new aspects, they are omitted here to reduce the number of indices and summation signs in the formulae. Also for simplicity we shall restrict the discussion to a system with tensors of coincident axial hyperfine symmetry as is found for a species undergoing fast uniaxial rotation. This is characterized by the Hamiltonian

$$\hat{H}/h = \nu_e\hat{S}_z - \nu_\mu\hat{I}^\mu_z - \nu_k\hat{I}^k_z + A^\mu_{iso}\hat{S}_z\hat{I}^\mu_z + A^k_{iso}\hat{S}_z\hat{I}^k_z + \tfrac{1}{2}A^\mu_{iso}[\hat{S}_+\hat{I}^\mu_- + \hat{S}_-\hat{I}^\mu_+] + \tfrac{1}{2}A^k_{iso}[\hat{S}_+\hat{I}^k_- + \hat{S}_-\hat{I}^k_+] + D^\mu_\perp[A + B + C + D + E + F] + D^k_\perp[A + B + C + D + E + F], \quad (2)$$

where $\nu_{e,\mu,k} = \gamma_{e,\mu,k} \times B_0$ are the electron, muon, and nuclear Zeeman frequencies in terms of their gyromagnetic ratios and the external field $\vec{B}_0$. $\hat{S}$, $\hat{I}^{\mu,k}$ are the corresponding spin operators, $A^{\mu,k}_{iso}$ their Fermi contact interaction and

$$D^{\mu,k}_\perp = -\frac{1}{2}D^{\mu,k}_\parallel = -\frac{\gamma_e\gamma_{\mu,k}h}{4\pi^2}\left\langle\frac{1}{r^3}\right\rangle \quad (3)$$

the principal components of the tensor describing the magnetic dipole interaction of the muon (nuclear) point-dipole with the unpaired electron which is smeared out in its orbital which is often the p_z-type. In polar coordinates the terms $A - F$ take the form[10]

$$\begin{aligned} A &= (1 - 3\cos^2\theta)\hat{S}_z\hat{I}^{\mu,k}_z \\ B &= -\tfrac{1}{4}(1 - 3\cos^2\theta)[\hat{S}_+\hat{I}^{\mu,k}_- + \hat{S}_-\hat{I}^{\mu,k}_+] & \Delta M &= 0 \\ C,D &= -\tfrac{3}{2}\sin\theta\cos\theta e^{\mp i\phi}[\hat{S}_z\hat{I}^{\mu,k}_\pm + \hat{S}_\pm\hat{I}^{\mu,k}_z] & \Delta M &= \pm 1 \\ E,F &= -\tfrac{3}{4}\sin^2\theta e^{\mp 2i\phi}\hat{S}_\pm\hat{I}^{\mu,k}_\pm & \Delta M &= \pm 2 \end{aligned} \quad (4)$$

where ϕ is the azimuthal angle, θ is the angle between the unique axis and $\vec{B}_0$, and $M = m^s + m^\mu + m^k$ is the quantum number for the z-component of the total angular momentum. The selection rules used referred to in this work are characterized by ΔM. They follow immediately from the structure of the operators. Note that operators of the type $\hat{S}_+\hat{I}_-$ and $\hat{S}_-\hat{I}_+$ which correspond to $\Delta M = 0$ arise both from dipolar (term B) and from isotropic interaction (equation 2).

Electron g-factor anisotropies are usually small but significant in organic radicals. Despite this, the electron Zeeman term was written as a scalar in the Hamiltonian. While this is not normally correct it is justified for μSR applications at high external fields where, as will be seen later, the electron Zeeman term cancels out in all relevant expressions to first order since we observe pure muon (nuclear) transitions.

2.2 The Basis for an Investigation of Reorientational Dynamics

Owing to the nature of the dipolar magnetic interaction the hyperfine coupling tensor has a fixed orientation with respect to the radical. It provides the handle for the study of reorientational dynamics since any motion which is fast compared with the inverse anisotropy leads to partial or complete averaging of the anisotropy. Little advantage of this fact has been taken hitherto to investigate radical motion.

Interaction between two point-dipoles depends on the angle θ between the line connecting the two dipoles and the direction of the external magnetic field, and it is proportional to $(3\cos^2\theta - 1)$. It is well known that for protons in the α-position to the radical centre the positive component of the dipolar interaction lies in the direction of the connecting bond, and that it adopts a value of + 30MHz for the malonyl radical.[10] The component parallel to the p_z-orbital is close to zero, and the third one therefore − 30 MHz.

The situation for β-protons is slightly more complicated since their position is usually not fixed to the nodal plane. As is shown in Figure 1, the two lobes of the p_z-orbital containing the unpaired electron are best accommodated in the positive cone of the function $(3\cos^2\theta - 1)$ when the external field $\vec{B}_0$ is close to parallel to the line connecting the β-nucleus with the radical centre. The two other components are negative, and it is found experimentally that they are often of the same magnitude so that the coupling tensor is approximately axial, with $D_\parallel$ pointing from the nucleus to the radical centre. Also, because of the $\langle r^{-3}\rangle$ dependence, it is reduced in magnitude compared with that for α-nuclei. $D_\parallel$ for β-protons in rigid, localized radicals is found to be typically + 7.5 MHz.

Any fast motion averages partly the hyperfine anisotropy.

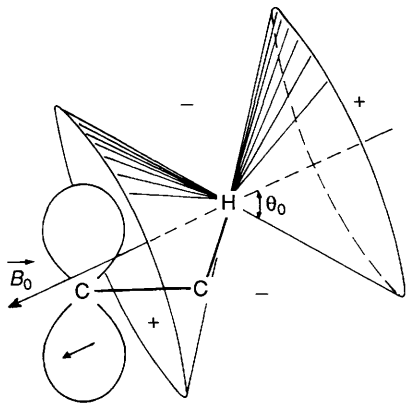

Figure 1 Dipolar interaction of the hydrogen nucleus in β-position, a point-dipole, with the unpaired electron which is 'smeared out' in a p_z-orbital. The orientation of the cone function $(3\cos^2\theta - 1)$ is shown for the situation when the magnetic field is roughly parallel to the direction of the positive component of the hyperfine anisotropy tensor. $\theta_0 = 54.7°$ is the magic angle where the dipolar coupling disappears.

Specifically, rotation about an axis perpendicular to $D_\parallel$ makes $D_\perp$ the new $D'_\parallel = -0.5D_\parallel$, *i.e.* the motion reduces the anisotropy by a factor of two and changes its sign. On this basis, recent quantitative analysis of anisotropic ESR spectra gave evidence for rotational motion of the tetramethylethylene radical cation in ZSM-5 zeolite.[11]

2.3 Evolution of Spin Polarization

The time evolution of muon polarization, $P(t)$, in the presence of a static external field has been evaluated previously using a density matrix approach.[12] Expressed in a basis of Zeeman product states, $\psi_m = \sum_i c_{im}\chi_i$, it is obtained for transverse fields as the expectation value of the Pauli spin operator $\langle\hat{\sigma}^\mu_x\rangle$, which leads to:

$$P_x(B_0,t) = \frac{2P^0_x}{N}\sum_m\sum_{n<m}\left|\sum_{i,j}c^*_{im}c_{jn}\langle\chi^\mu_i|\hat{\sigma}^\mu_x|\chi^\mu_j\rangle \times \delta^e_{ij}\delta^k_{ij}\right|^2 \cos(2\pi\nu_{nm}t)e^{-\lambda t}. \quad (5)$$

For longitudinal fields $\langle\hat{\sigma}^\mu_z\rangle$ gives

$$P_z(B_0,t) = \frac{4P^0_z}{N}\sum_m\left(\left|\sum_i c^*_{im}c_{im}m^\mu_i\right|^2 + 2\sum_{n<m}\left|\sum_i c^*_{im}c_{in}m^\mu_i\right|^2\cos(2\pi\nu_{nm}t)e^{-\lambda t}\right). \quad (6)$$

$P^0_{x,z}$ is the initial muon polarization of the species of interest, $N = 4\Pi_k(2I^k + 1)$ the dimension of its energy matrix, $\delta^{e,k}_{ij} = \langle\chi^{e,k}_i|\chi^{e,k}_j\rangle$ the Kronecker delta, and $\lambda = \lambda_0 + \lambda'$ represents the relaxation on the transition frequency $\nu_{nm} = (E_n - E_m)/h$. $\lambda_0 = 0.4551\ \mu s^{-1}$ is the inverse muon life time and λ' is the first-order rate constant which accounts for chemical reaction into a state with different resonance conditions.

2.4 Simplification in Zero Magnetic Field

In the absence of an external magnetic field the Zeeman terms in the Hamiltonian vanish. Furthermore, the energy spectrum of the system is independent of its orientation in a laboratory frame. While conventional magnetic resonance usually avoids zero field conditions, μSR has taken advantage of the unique situation for isotropic systems with equivalent nuclei,[12] or for anisotropic systems in the absence of magnetic nuclei.

The simplest system is that of a muon–electron two-spin-$\frac{1}{2}$ system. In the isotropic case, three of the four eigenstates form a degenerate triplet which is separated by A^μ_{iso} from the singlet state. Spin polarization oscillates between muon and electron, and the only non-zero frequency is expected at A^μ_{iso}. This

corresponds to 4463 MHz for vacuum-like Mu and needs special experimental effort to resolve, while the reduced hyperfine interaction in radicals is more easily accessible In the presence of axial anisotropy, the triplet splits into a doublet and another singlet Three frequencies at $A^{\mu}_{iso} - 2D^{\mu}_{\perp}$, $A^{\mu}_{iso} + D^{\mu}_{\perp}$, and $3D^{\mu}_{\perp}$ are expected for this case In Section 4 1 3, Mu@C_{70} will serve as an example for this case

The situation becomes immediately more complex when further magnetic nuclei are present It is no longer possible to read coupling constants directly off the spectrum For the case of an arbitrary number of equivalent protons in addition to muon and electron, however, it has been possible to work out analytical expressions for frequencies and transition amplitudes [12] The case will be treated further in Section 3 1 and is illustrated in Figure 5

2.5 General Behaviour in High Magnetic Fields

Because of the simplification of spectra it is convenient, as in magnetic resonance in general, to work in high fields where $\nu_e \gg A^{\mu}_{iso}, A^{k}_{iso}$ Except for the special conditions encountered near avoided crossings of energy levels, the muon is then decoupled from the other magnetic nucleus Eigenstates ψ are pure individual product states χ_i, *i e* the expansion coefficients c_{im} in equations 5 and 6 take the values 0 and 1

In *longitudinal* fields, the time dependence vanishes, and the muon polarization $P_z(B_0\ t) = P^0$ becomes static The time dependence in *transverse* fields is governed by $\hat{\sigma}^{\mu}_{x}$ (see equation 5) which mixes states which differ in the muon but not in the electron or nuclear spin quantum number This is expressed by the selection rules $|\ \Delta m^{\mu}\ | = 1$, $\Delta m^{s\,k} = 0$ The corresponding transition frequencies are given to first order by

$$\nu_{\pm} = |\nu_{\mu} \pm \tfrac{1}{2}[A^{\mu}_{iso} + D^{\mu}_{\perp}(1 - 3\cos^2\theta)]| \qquad (7)$$

More accurate expressions are found in the specialized literature [12 13]

The frequencies correspond to the two ENDOR transitions of the muon in the radical Because of the high field condition they are independent of nuclear Zeeman or hyperfine terms, each line is therefore degenerate by a factor $(2I^k + 1)$ and has an amplitude of $0\ 5P^0_x$ The line shape is given by the Fourier transform of the exponentially damped cosine functions in equation 5, which is a Lorentzian with full width at half maximum 2λ The muon hyperfine parameter is obtained directly as the sum (or difference, depending on the relative magnitude of the terms in equation 7) of the two frequencies In polycrystalline material the distribution of θ-values leads to powder patterns of asymmetric shape

2.6 Behaviour at Avoided Level Crossings (ALCs)

The theory for ALC resonances of isotropic systems containing a spin polarized muon has been developed by Heming *et al* [14] and extended to more general cases in solids by Kiefl [15] and by Roduner [16] Dynamic effects have also been treated [17 18] Only a brief outline is given here

At true crossings of magnetic energy levels in high fields, eigenstates are pure Zeeman product states, but near avoided crossings they are mixtures of the two crossing states The normal high field approximation is thus no longer valid This leads to a broadening or even to a splitting of one of the transverse field lines [15] In longitudinal fields too, the system is not prepared in an eigenstate, and it therefore oscillates at a frequency given by the energy difference between the two mixing states In the time-integrated forward–backward decay asymmetry this leads to a resonance at the field which meets the ALC condition As can be seen by inspection of the Hamiltonian and in particular of equation 4, there are three types of resonances, characterized by the selection rules $|\Delta M| = |\Delta(m^{\mu} + m^{k})| = 0, 1, 2$ The resonance field is given to first order by

$$B_r = \left| \frac{A^{\mu}_{iso} - D^{\mu}_{\perp}(1 - 3\cos^2\theta) + (|\Delta M| - 1)[A^{k}_{iso} - D^{k}_{\perp}(1 - 3\cos^2\theta)]}{2[\gamma_{\mu} + (|\Delta M| - 1)\gamma_k]} \right| \qquad (8)$$

Higher order terms have to be taken into account for quantitative work, but the corrections are usually on a level < 1% The amplitude as a function of field is determined from the time integral of equation 6 The field dependence of the expansion coefficients c_{im} leads to resonances of Lorentzian shape which are broadened in the presence of relaxation or chemical reaction In polycrystalline material the different orientations lead again to powder patterns

The three types of avoided crossings are shown in the energy level diagram of Figure 2 Outside the resonances, the energies vary linearly with magnetic field, and the states are pure Zeeman states as indicated by the labelling Only the four states with electron spin α are shown, the others are well separated in energy

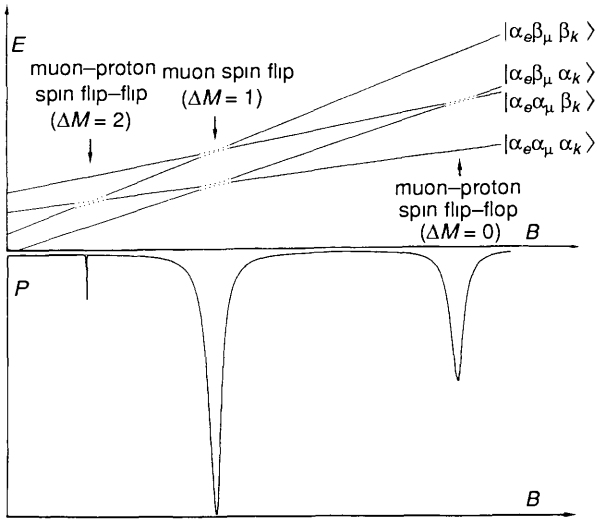

Figure 2 High-field energy level diagram for a three-spin system of an electron *e*, positive muon μ, and proton *k* Muon avoided level crossing resonances occur when states with opposite muon spins become near-degenerate in energy, allowing the system to oscillate between them

The simplest case is the $\Delta M = 1$ ALC line Two states which belong to the same electron and nuclear spin but differ in the muon spin are mixed by operators of the form $\hat{S}_z\hat{I}^{\mu}_{\pm}$ The elements *C* and *D* of the Hamiltonian (equations 2 and 4) are of this form They are non-zero in the presence of muon hyperfine anistropy (except for the special orientations $\theta = n\pi/2$ for integer *n*) Muon hyperfine anisotropy therefore leads to an avoided crossing of this type, but in the absence of anisotropy the levels are not mixed, and the corresponding resonance will be absent The resonance is therefore especially suitable to study anisotropic reorientational motion of radicals in orienting environments, even in polycrystalline or amorphous states [19] The critical time for the averaging process is given by the inverse anisotropy, $D^{\mu}_{\perp}$

The $\Delta M = 0$ line, a muon–nuclear spin flip–flop transition, is allowed only in second order, since the Hamiltonian provides no direct matrix elements which mix the two Zeeman states The degeneracy at the crossing is lifted by *isotropic* coupling of the two states to a third, distant state with opposite electron spin ($|\beta_e\alpha_{\mu}\alpha_{\kappa}\rangle$ for the case shown in Figure 2), and the active element is $A^{\mu}_{iso}\hat{S}_+\hat{I}^{\mu}$ combined with $A^{k}_{iso}\hat{S}_-\hat{I}^{\mu}_{+}$ Resonances of this type are observed also in liquids where rapid tumbling averages the anisotropy to zero Inspection of equation 8 shows that the resonance position depends on the relative sign of the muon and the nuclear hyperfine interaction terms Since the radicals are formed in a way which leaves the muon in a position of the molecule where A^{μ}_{iso} is normally positive, it allows the determi-

nation of the sign of nuclear coupling constants, which is unique in magnetic resonance

The last type is the $|\Delta M| = 2$ muon–nuclear spin flip–flip transition The crossing is avoided again indirectly, as in the $\Delta M = 0$ case, but it occurs only in the presence of anisotropy (terms E and F in equation 4) It is usually weak and narrow and has therefore not found practical applications yet

3 Experimental Techniques

Several variants of experimental techniques have been developed They have in common that they all stop energetic muons of a spin polarized beam from an accelerator port in the sample to be investigated To monitor the signal they are all based on the detection of the decay positrons which are emitted preferentially along the instantaneous spin direction when the muon decays The first such experiment was reported by Garwin *et al* [20] in their verification of the parity violation in pion decay A scheme of the experimental set-up for the two main variants is shown in Figure 3 In both cases the muon enters from the left, with its spin polarized in the direction of flight, and the decay positrons are detected by a set of scintillation counters which surround the sample placed in the centre of a magnet The scintillator pulse sequences are logically analysed in a fast electronics, and good events are stored in a multi channel analyser or computer memory in the form of a time histogram or field scan as shown in the insets

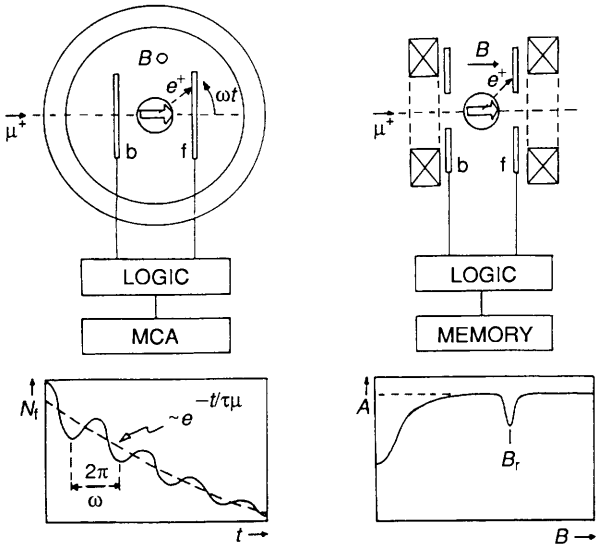

Figure 3 Block scheme of apparatus for time-resolved transverse field muon spin rotation (TD-μSR, left) and for time-integrated longitudinal field avoided level crossing resonance (ALC-μSR, right)

3.1 Time Differential Muon Spin Rotation (TD-μSR)

The left-hand side of Figure 3 shows the set-up for TD-μSR It is used most often in transverse but occasionally also in longitudinal or even in zero external magnetic field The incoming muon triggers the backward counter b and starts the clock for a lifetime measurement The decay positron, if detected in the forward counter f, stops this clock Good events are counted in the proper channel of the histogram Bad events, in particular those where more than a single muon has been detected in the sample during a time window of several microseconds, are eliminated by the logical circuit The principal content of the histogram is a radioactive decay curve which corresponds to the muon lifetime The muon precesses in a transverse magnetic field, and therefore the detection probability for decay positrons sweeps past the forward counter, which leads to a modulation of the decay curve with the muon precession frequencies This superimposed signal, represented by equation 5, is the analogue of a free induction decay following a $\pi/2$ pulse for a selected nucleus in Fourier transform magnetic resonance As in NMR, it is often the Fourier transformed FID rather than the raw time histogram which is displayed

An instructive set of TD-μSR frequency spectra, obtained with a sample of liquid vinylene carbonate in various magnetic fields, is shown in the Figures 4 and 5 In a high transverse field (1600 Gauss, top of Figure 4) we observe three frequencies The intense line ν_μ at 21 7 MHz is due to muons which have come to rest in a diamagnetic environment and therefore precess at the muon Zeeman frequency of 13 55 kHz/Gauss Owing to the short muon lifetime chemical shifts or nuclear couplings are not resolved so that this signal usually has to be assumed to be a superposition of contributions arising from muons in various environments For the present case, it is plausible to assume that it represents muons which have been trapped in the lone pairs of the oxygen atoms Alternatively, one can imagine that a Mu atom has substituted a hydrogen atom in the molecule in a hot atom reaction, or that it has abstracted H so that the muon is actually present as MuH A pair of lines R corresponds to the radical formed by Mu addition to the double bond of the molecule They are centred at $\frac{1}{2}A^{\mu}_{iso} = 178\ 7$ MHz, and displaced approximately by ν_μ as is seen in equation 7 for the isotropic case with $D^{\mu}_{\perp} = 0$ The higher of the two frequencies has a lower amplitude as a consequence of the limited time resolution of the experiment The muon hyperfine coupling constant, $A^{\mu}_{iso} = 357\ 5$ MHz, is obtained directly by taking the sum of the two frequencies

The second spectrum was obtained in a field of 117 Gauss where the high field condition for muon decoupling from the protons no longer applies The radical lines are still centred at $\frac{1}{2}A^{\mu}_{iso}$, but they are much further apart, and each line is split into a doublet of doublets by the two protons By numerical diagonalization it is possible to derive from the line positions sign and magnitude of the two proton coupling constants (here − 39 8 MHz for the α-proton and 98 4 MHz for the β-proton) The most general case is found for a field of 20 G, which corresponds to about the proton hyperfine fields at the electron The muon polarization is now distributed over 56 transitions of different intensities, which leaves very little for an individual line A

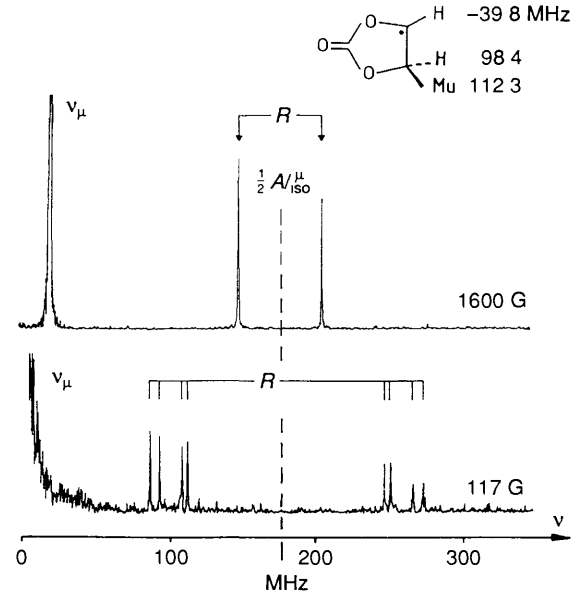

Figure 4 TD-μSR spectrum obtained with liquid vinylene carbonate at 300 K in a magnetic field of 1600 Gauss (top) and 117 Gauss (bottom) ν_μ is the Zeeman frequency for muons in diamagnetic environments R is a pair of lines arising from radicals formed by Mu addition to the vinylene double bond The numbers next to the formula are the hyperfine coupling constants, which for the muon has been reduced by a factor $\mu_\mu/\mu_p = 3\ 1833$ to make it directly comparable to the proton value

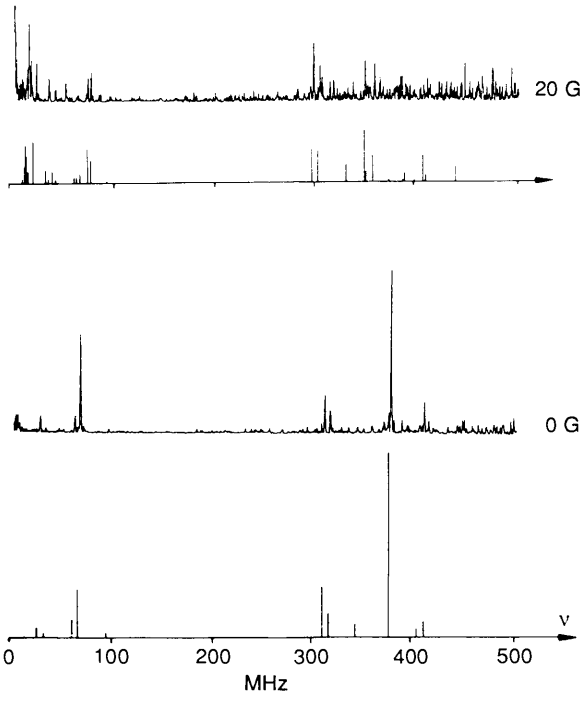

Figure 5 Simulated and observed TD-μSR spectra of the Mu adduct to vinylene carbonate in a low transverse and in zero field The apparent increased noise level at high frequencies is a consequence of a deconvolution for instrumental time resolution

comparison between simulation and experiment gives satisfactory agreement (top of Figure 5) A more favourable situation is attained in zero field, where because of degeneracy of states the number of transitions reduces to 12 only (bottom of Figure 5) The example demonstrates that it is possible in simple cases to extract from a zero field spectrum the entire information on coupling constants This option is particularly attractive for powders which normally give rise to broad lines in an external field – in zero field they are expected to give single crystal like features

Reduction of A^{μ}_{iso} by the muon–proton relative magnetic moments, $\mu_{\mu}/\mu_{p} = 3\ 1833$, gives a value of 112 3 MHz, which compared to the 98 4 MHz for the proton in the equivalent position reveals a hyperfine isotope effect of 14% This effect has been ascribed to the length of the C–Mu bond which in the dynamic average of a Morse oscillator exceeds that of an equivalent C–H bond by nearly 5% [21]

3.2 Time Integral Avoided Level Crossing Muon Spin Resonance (ALC-μSR)

The right-hand side of Figure 3 shows the ALC-μSR set-up in a longitudinal magnetic field The incoming muon is not detected, only the decay positrons are counted in the two detectors f and b There is thus no principal limit on the muon flux as in the case of TD-μSR The field is scanned in small steps, and for each field value the muon polarization is measured It is proportional to the experimental asymmetry $\mathscr{A}$, where

$$\mathscr{A} = \frac{N_f - N_b}{N_f + N_b}, \qquad (9)$$

and $N_{f,b}$ are the total number of positrons counted in the two counters

Figure 6 displays a typical example of an ALC-μSR spectrum It was obtained with a liquid solution of 6,6-dimethylfulvene in diethyl ether [22] Eight clear resonances are resolved, which because of the liquid state are all of the type $\Delta M = 0$ A TD-μSR experiment of the same fulvene revealed two radicals with $A^{\mu}_{iso} = 105\ 1$ MHz and 203 4 MHz, and with relative yields of 60% and 40%, respectively Analysis of the resonance positions is based on equation 8 which for the isotropic case and when the nuclei are protons reduces to $B_r = |A^{\mu}_{iso} - A^{k}_{iso}| \times 53\ 80$ Gauss, with $A^{\mu,k}_{iso}$ given in MHz It shows that the two radicals appear separated in the ALC spectrum, and that the first resonance from the left is composed of two near-degenerate lines The two structures and the assignment of the coupling constants, which are entirely consistent with expectation for radicals of a pentadienyl type and of a cross-conjugated allyl radical, are given on top of the figure A simulation is in excellent agreement with the experimental spectrum The dividing lines between resonances of positive and of negative proton couplings is indicated It should be noted that smaller couplings lead to less intense and often unobserved resonances, so that a typical gap is normally observed around the dividing lines Furthermore, the line width is proportional to $|A^{\mu}_{iso} - A^{k}_{iso}|^{-1}$ so that negative proton couplings normally lead to narrower lines, which can be used as a further help for the assignment The hyperfine isotope effect between the muon and the proton bound to the same carbon atom amounts again to *ca* 14%, as was found and discussed above for the case of vinylene carbonate

Comparison of TD-μSR with ALC-μSR shows that the two techniques are to some extent complementary Since the selection rules are different, one obtains different information Of the hyperfine parameters, high transverse fields yield only the muon coupling constant, whereas the ALC technique gives in isotropic media the muon–nuclear difference When radicals are too complex to allow the observation of zero-field spectra, then the total information is obtained in a single experiment only from an ALC spectrum recorded under frozen conditions so that A^{μ}_{iso} is obtained from a $\Delta M = 1$ type transition

Integration in ALC spectroscopy removes the constraint which allows only a single muon in the sample at any given time It thus profits from the higher muon fluxes which have become available This is at a cost of the direct information about the time dependence It is often advisable to do both types of experiments If details of the relaxation function in longitudinal fields need to be known it is of course possible to combine the two experimental philosophies, and to do a time resolved longitudinal experiment A further advantage of longitudinal fields is the absence of transverse relaxation processes (T_2) This usually simplifies things, and in the case of slow radical formation from the Mu precursor it avoids the loss of phase coherence and makes it possible that radicals can be observed which are formed in a microsecond instead of a nanosecond This should make a whole new class of radicals accessible to observation

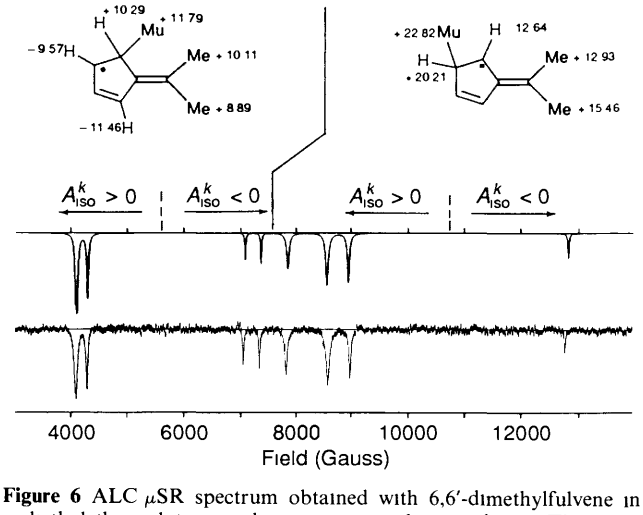

Figure 6 ALC μSR spectrum obtained with 6,6′-dimethylfulvene in diethylether solution, and comparison with a simulation The structures of the two radicals with the coupling constants (converted to Gauss) are given on top

4 Applications to Problems of Current Interest

4.1 Reorientation Dynamics in Solids

4 1 1 ALC-μSR of a Benzene Single Crystal

The dynamics of benzene have been investigated in detail by NMR The dominating motion, a jump reorientation about the sixfold axis of the molecule, has an Arrhenius frequency factor of 1 09 × 10^{14} s^{-1} and an activation energy of 17 6 kJ mol^{-1} [23]

Figure 7 displays an ALC-μSR spectrum of frozen benzene at 263 K Based on the known isotropic coupling constants from work in the liquid phase the three resonances are easily assigned to the strong $|\Delta M| = 1$ feature, and to the two transitions with $|\Delta M| = 0, 2$ arising from indirect interaction of the muon with the methylene proton Further $|\Delta M| = 0$ lines are present at higher fields but outside the range of the figure The inset shows a scan with increased resolution and on an expanded scale over the very narrow $|\Delta M| = 2$ resonance which has a full width at half maximum of only 28 G All lines are of Lorentzian shape An excellent simulation is obtained with isotropic hyperfine parameters A^{μ}_{iso} = 519 7 MHz, A^{k}_{iso} = 126 5 MHz, with corresponding anisotropies $D^{\mu}_{\perp}$ = 3 5 MHz and $D^{k}_{\perp}$ = 0 9 MHz, and with an angle of $\theta = 80°$ between the external magnetic field and the hyperfine symmetry axis Both, the width of the $|\Delta M| = 1$ and the intensity of the $|\Delta M| = 2$ line, are strongly orientation dependent and leave an uncertainty of only 2° for θ

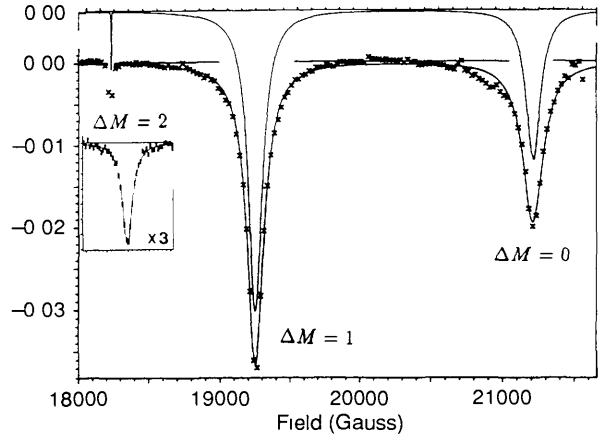

Figure 7 Experimental spectrum obtained with frozen benzene at 263 K and simulation of a single crystal spectrum for a cyclohexadienyl radical with coaxial hyperfine interactions of A^{μ}_{iso} = 519 7 MHz $D^{\mu}_{\perp}$ = 3 5 MHz for the muon and A^{p}_{iso} = 126 5 MHz, $D^{p}_{\perp}$ = 0 9 MHz for the corresponding methylene proton The angle between the hyperfine axis and the external field is 80° The inset shows the $\Delta M = 2$ transition with the field axis expanded by a factor of three and the asymmetry axis by a factor of two

Both, the muon and the proton, are bound to the methylene carbon and thus chemically equivalent It should be noted that equation 8 predicts degeneracy of the three transitions for the case where the corresponding hyperfine couplings scale with the muon–proton ratio of the magnetic moments The fact that they are well separated in the experimental spectrum is a direct visualization of the hyperfine isotope effect

Observation of such a simple spectrum for simply frozen benzene is striking, considering the fact that crystalline benzene has four molecules with different orientations per unit cell, and that each molecule has twelve sites (six from each side) available for Mu addition The complexity of the situation has been demonstrated previously for the related case of a naphthalene single crystal which gives orientation-dependent multi-line TD-μSR spectra [24] In the present case, the observed spectrum is compatible with expectation only for the conditions of fast rotation of the radicals in the crystal, *and* with the presence of a *single* crystal which has the crystallographic *b* axis parallel to the external field so that all four orientations become equivalent The condition of fast rotation is expected to apply, as NMR results give a correlation time for jump rotation of 28 ps at this temperature Furthermore, it is known that benzene often forms single crystals on simple cooling The special alignment of the crystal was not always reproducible in further experiments, but it is plausible that the presence of a high magnetic field or the shape of the sample cell initiated a preferred orientation

On cooling, the resonances broaden considerably, and at 163 K there is an indication of developing structure, but the signal also becomes very weak due to the reduced fraction of muons which end up in the radical The theory for quantitative analysis of these data has not yet been worked out, but it is obvious that they bear dynamic information

4 1 2 The Plastic Phase of Polycrystalline Norbornene

Norbornene is a near-globular molecule, and as a typical member of that family it exhibits a plastic solid phase with fast rotations of the molecules It has a hexagonal crystal structure between 129 K and the melting point at 320 K, and its reorientational dynamics have been investigated by means of depolarized Rayleigh scattering and NMR spin–lattice measurements No indication of any anisotropy was found, and correlation times of the order of 10^{-11} s were derived, with no discontinuity at the phase transition to the liquid TD-μSR measurements using a single crystal revealed an orientation dependence of the hyperfine interactions of the *exo* and the *endo* Mu adduct radicals and yielded the first evidence of anisotropic motion [25] Large single crystals are difficult to obtain for many materials The potential of ALC-μSR was therefore tested using polycrystalline norbornene

Figure 8 displays the $\Delta M| = 1$ resonance of the *exo* Mu adduct Similar lines were observed for the isomer with Mu in the *endo* position The resonance field is directly proportional to the muon hyperfine coupling and according to equation 8 scales as $B_r = A^{\mu}_{iso} \times 36\ 90$ Gauss The mere presence of these lines is proof for anisotropy of the motion on a time scale of $(2\pi D_{\perp})^{-1}$ At the lower temperatures the shape of the features is clearly asymmetric and agrees with expectation for a powder The fact that the steep flank is on the high-field side of the resonance shows that orientations with effective hyperfine couplings larger than the isotropic value occur more often Since A^{μ}_{iso} is positive it means that $D^{\mu}_{\perp}$ is also positive This immediately excludes the possibility that the unique axis of rotation is approximately

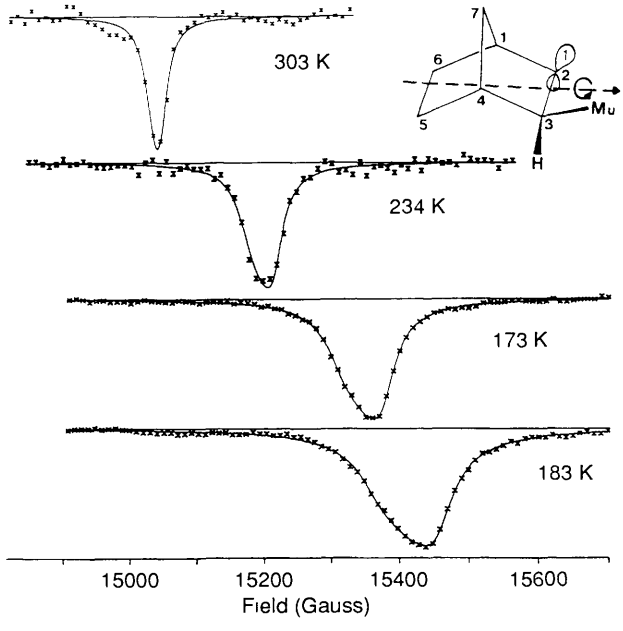

Figure 8 ALC-μSR spectra obtained with polycrystalline norbornene in the plastic phase Displayed is the $\Delta M| = 1$ resonance corresponding to the Mu adduct in the *exo* position of the double bond of norbornene

parallel to the line connecting atoms C_1 and C_4 and thus contradicts the original proposal.[26] Analysis of the anisotropy of the $\Delta M = 0$ resonances (which are not shown here) reveals that this unique axis is most likely roughly parallel to the line C_2—C_6, as indicated in the structural formula in Figure 8.

The width of the powder patterns in Figure 8 is directly related to the muon hyperfine anisotropy. The corresponding parameter from a fit of the theoretical line shape function agrees quantitatively with the result obtained from the single crystal TD-μSR experiment, and this is encouraging in view of future ALC-μSR experiments with powder materials since single crystals of suitable size are often not available.

It is of interest to obtain information about the type of motion of the radical or molecule in the crystal. For near-spherical species one might expect small-angle rotational diffusion. Recent theoretical work shows that onset of such a motion leads to *broadening* of a $|\Delta M| = 1$ resonance, and eventually to its disappearance at high temperatures as a very broad feature.[18] This is not what we observe. The line *narrows* as temperature increases, and the shape is the same as that of a static axial system with reduced effective hyperfine anisotropy. The averaging process must be fast on the experimental time scale, and the amplitude of the averaging motion must increase with temperature. Some sort of precessional jumps rather than rotational diffusion could explain the observed behaviour.

4.1.3 *Probing the Dynamics of Solid C_{70} Fullerene*

C_{70} is an ellipsoidal molecule which in the solid state could well be expected to form a plastic phase with the molecule reorienting in some way, but little is known about it so far. Molecular dynamics calculations reveal a complicated structural behaviour, associated with the presence of the anisotropy of the molecule. Being one of the materials which is available in high purity only in small amounts and not in single crystals, and considering the fact that Mu adds by addition to form radicals,[26] C_{70} is an attractive candidate for study of its dynamics by means of ALC-μSR. Such an experiment has been carried out and is currently being analysed. Reorientational disorder of C_{70} sets in gradually, in a manner which is much the same as in norbornene. There must be a fast averaging process such as, for example, the precessional motion which has been predicted by the molecular dynamics calculations.[27]

Besides Mu adduct radicals, endohedral Mu was also detected with fullerenes, and it appeared to relax at the lower temperatures much more rapidly in C_{70} than in C_{60},[26] which was taken as evidence that Mu@C_{70} is sensitive to the anisotropy of the cage. This was verified in zero field experiments. Example spectra are displayed in Figure 9. A fraction of the muons relax at close to zero frequency, but at 200 K a clear peak is observed at $\frac{3}{2}D_{\perp}^{\mu} = 0.76$ MHz as expected for axial anisotropy

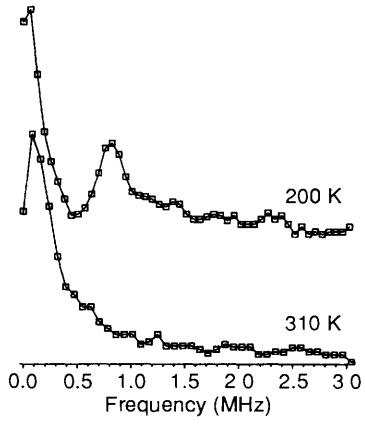

Figure 9 Fourier transform amplitude in arbitrary units of histograms measured with C_{70} in zero external magnetic field at two temperatures The peak at 0 76 MHz is proof for anisotropic Mu

(see Section 2.4) while the time resolution was not sufficient to detect also the high frequencies.[28] Interestingly, this peak disappears at the phase transition at 270 K, which shows that above this temperature the fullerene cages reorient fast enough to make the system appear isotropic.

The anisotropy can be described by admixture of *ca.* 1% of $2p$ character to the $1s$ wave function. The resulting electron density distribution for Mu placed in the centre of C_{70} is shown in Figure 10. The spherical $1s$ contribution dominates in the centre but damps away more quickly than the $2p$ so that a slightly pinched shape is obtained which fits the cage walls very well. The anisotropy may be a consequence of the shape of the C_{70} cage or of the pronounced charge distribution which according to semi-empirical calculations leaves a pronounced positive charge at the equator carbon atoms. By locking to the orientation of the cage the Mu atom can monitor the reorientational dynamics of the fullerene. The increase in energy by $2p$ admixture is comparable to the zero-point vibrational energy for the three-dimensional harmonic oscillator of the endohedral atom in the van der Waals potential of the cage.[28]

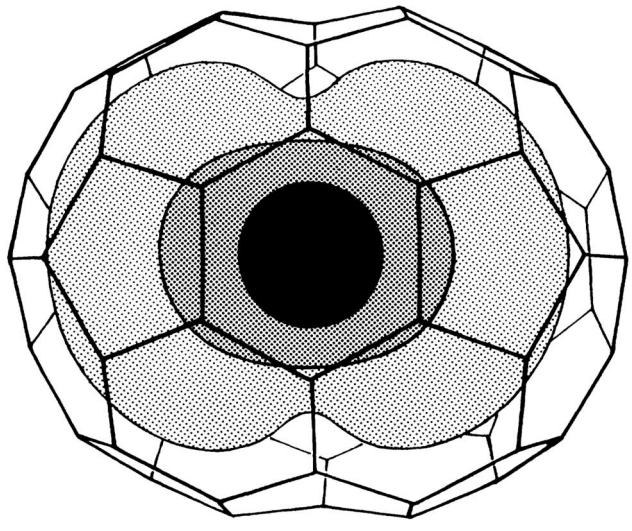

Figure 10 Electron density contour map of Mu@C_{70} The Mu wave function is represented by $\Psi_{Mu} = 0\ 9954\Psi_{1s} + 0\ 0959i\Psi_{2p_z}$ The contours represent values equal to 10^{-3}, 10^{-5}, and 10^{-7}, of the electron density at the muon

4.2 Diffusion and Reorientation Dynamics of Radicals on Surfaces

Organic free radicals on surfaces can be observed by ESR at low temperatures, where their dynamics are frozen. As soon as mobility sets in termination reactions lead to the disappearance of the radicals, and the signal is lost. Conditions are more favourable in porous silica and in zeolites, where pores and cages hinder translational diffusion.

Because of the high sensitivity, the μSR techniques can detect radicals at ultra-low concentrations where termination does not play a role. Observation is possible even at elevated temperatures which are more relevant to chemistry. Figure 11 shows an ALC-μSR spectrum of the cyclohexadienyl radical observed at 334 K on muon irradiation of a sample of spherical fused silica grains of 7 nm diameter covered with a nominal monolayer of benzene. Three beautiful resonances are detected. They are all of the $\Delta M = 0$ type and involve the nuclei indicated by the arrows. The isosteric heat of adsorption of benzene on a hydroxylated silica surface amounts to *ca.* 43 kJ mol^{-1} and is considerably larger than the heat of vaporization of the liquid (34 kJ mol^{-1}). Benzene therefore condenses and spreads on the surface and does not form droplets or escape into the vapour phase. The radical is expected to behave the same way, and the fact that the resonance positions are shifted slightly to higher fields compared with the liquid supports further the conclusion that the radical is

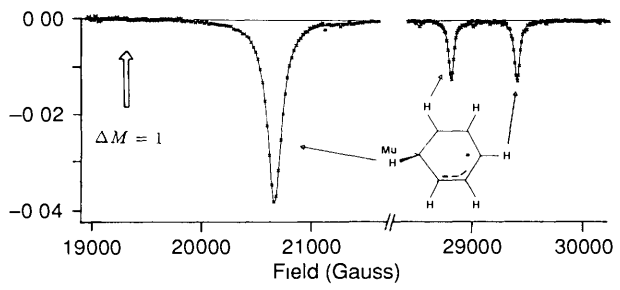

Figure 11 ALC spectrum obtained with a mono layer of benzene on spherical SiO_2 grains (Cab-O-Sil EH-5) of 7 nm diameter at 334 K Only $\Delta M = 0$ resonances of the cyclohexadienyl radical are observed, and the arrows assign the protons involved

adsorbed on the surface This certainly leads to a preferred orientation, and it is known that benzene molecules lie flat on hydroxylated surfaces The radical should thus display anisotropic behaviour, and we expect to find a $|\Delta M| = 1$ resonance In contrast, the resonances are all of ideal Lorentzian shape, not much broader than in the bulk liquid, and there is not the slightest indication of a $|\Delta M| = 1$ line (heavy arrow in the figure)

The methylene proton signal was measured at twelve temperatures from 334 K down to 139 K, where it disappears [29] The line broadens continuously, but its shape remains Lorentzian at all temperatures The $|\Delta M| = 1$ resonance, which is the strongest in solid benzene (Figure 7), is detected as a very weak feature at best Both indicate that the conditions remain isotropic and that we are in the region of motional narrowing By translational diffusion on the surface of the spherical grain the radical samples all orientations and averages the hyperfine Hamiltonian Furthermore, it is likely that flipping over of the disk-shaped species contributes to the absence of this signal This motion leaves the Hamiltonian unchanged but in the case of the $|\Delta M| = 1$ resonance changes the sign of the term driving the transition It thus reverses time evolution of muon polarization A quantitative theory based on a stochastic Liouville approach has been developed[18] and used for the analysis of the experimental data Preliminary results show that the activation of diffusion and even the coefficient for translational diffusion is similar to that in the liquid at the corresponding temperature

Silica is often used as a support for metal catalysts It is therefore attractive to attempt observation of radicals, as potential transient intermediates of catalytic processes, adsorbed on the surface of real catalysts This is indeed possible Figure 12 shows the ALC-μSR spectrum obtained with a nominal 5% layer of benzene on the surface of a platinum loaded silica catalyst Because of the low coverage the signal is small, and therefore the derivative spectrum is displayed, but the three resonances which have been observed with plain silica (Figure 11) are clearly seen In addition, there is a small feature at the field where the $|\Delta M| = 1$ line is expected The resonance positions and thus the isotropic hyperfine interactions are the same as for plain silica at the corresponding temperature, even the line widths are close to the same This certainly comes as a surprise It makes clear that even though the radical is highly mobile and must diffuse fast enough to find the metal clusters, it is not influenced by their presence The platinum islands are obviously blocked by adsorbed benzene, and the radicals avoid these islands or skim over rapidly without taking notice of the metal under the insulating benzene layer

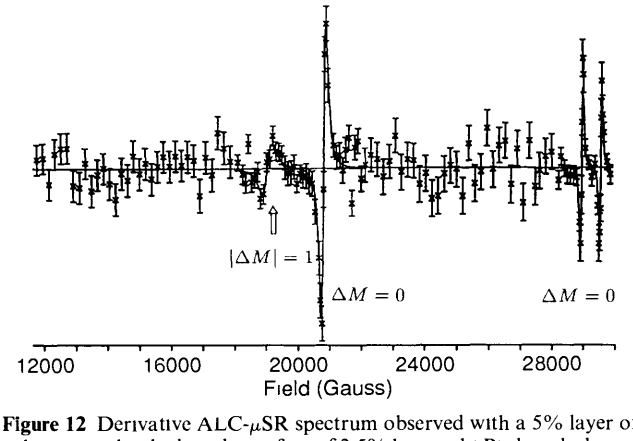

Figure 12 Derivative ALC-μSR spectrum observed with a 5% layer of benzene adsorbed on the surface of 2 5% by weight Pt-doped silica at 303 K

4.3 Organic Radicals in the Gas Phase

Radicals consisting of more than three to four atoms are not normally detectable in the gas by conventional magnetic resonance techniques, since the spectra are complex and the signal is split over too many lines to be observable For the techniques using highly polarized muons the situation is more favourable The ethyl radical has been observed at roughly atmospheric pressures using both the TD-μSR and the ALC-μSR techniques An example for the latter is shown in Figure 13 which gives the two $\Delta M = 0$ resonances for the ethyl radical in 1 5 bar pure ethylene, and with small amounts of oxygen added Due to the spin–rotation interaction the lines have a width of about 500 Gauss in the absence of oxygen This is more than an order of magnitude greater than in the liquid, but the resonances are still evident The radical reacts with oxygen chemically and by Heisenberg spin exchange, and this leads to further broadening Taking advantage of the fact that the two processes have a different effect on the line shape the method provides a tool to measure radical reaction rate constants and contributes to an understanding of gas phase processes which are of relevance in the photochemical degradation of organic pollutants in the atmosphere

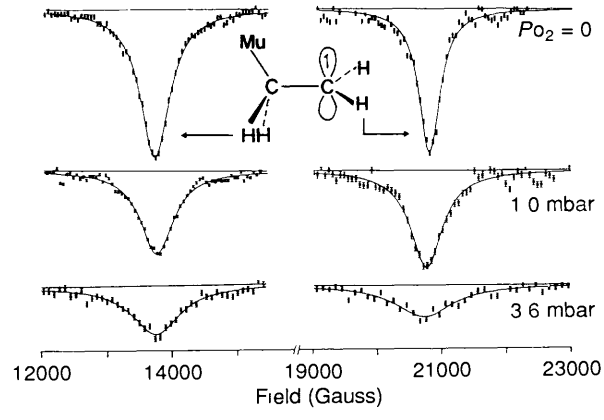

Figure 13 ALC μSR spectra obtained with 1 5 bar ethylene at three concentrations of oxygen The two resonances correspond to the selection rule $\Delta M = 0$ and belong to the α proton (20750 Gauss) and the β proton (13750) Gauss) of the muonated ethyl radical

5 Comparison with other Magnetic Resonance Techniques

Typical values for some of the important parameters which allow a comparison of μSR with ESR and NMR are given in Table 1 It is obvious that the principal advantage of μSR lies in the polarization of the muon beam, which is close to unity independent of temperature, whereas the other techniques normally have to work with Boltzman populations This is important, in particular at elevated temperatures, and in zero magnetic field Together with the short lifetime of the muon it has the consequence that the muon technique can work with extremely low radical concentrations of the order of twenty or even a single species in the entire sample at any given time Even the lowest concentration of a solute is thus not depleted by chemical

Table 1 Comparison of typical parameters in μSR, ESR, and NMR

	μSR	ESR	NMR
Polarization at 300 K	≈ 1 0	10^{-3}	10^{-5}
Minimum number of spins for simple spectrum	10^7	5×10^{10}	10^{17}
Frequency resolution	0 5 MHz	50 kHz	0 1 Hz
Time resolution	1 ns	20 ns	1μs

reactions during an experiment, and kinetics of bimolecular reactions are always of ideal pseudo-first order Also, self termination which imposes the principal limitation on radical concentrations for ESR experiments in solution, is absent

The muon lifetime of 2 2μs poses a principal limitation on the time scale of the processes to be studied by μSR It is responsible for the low frequency resolution which does not allow resolving chemical shifts and thus discriminating between different diamagnetic muonated species Only fast processes can be monitored, but it is of course exactly these which are usually the more difficult ones to study by conventional techniques

The limitation on the time resolution in ESR and NMR comes from the necessity to first create spin coherence using a high frequency preparation pulse Muons are injected into the sample already polarized Time resolution is determined by the rise time of photomultipliers and in particular by the size of scintillation counters, as the length of the light paths from muons triggering the counter in different places varies, and the distance travelled in one nanosecond is of the order of 20 cm in these materials

In NMR, and more and more frequently also in ESR, one takes advantage of elaborate pulse sequences Pulsed techniques have been applied and are still being investigated for μSR, but the muon lifetime again imposes a major limitation The muon magnetic moment is only three times that of a proton, so that it takes a significant fraction of the muon lifetime to tip it by 90°, even when high RF powers are applied The technique may develop an advantage on pulsed muon beams and for special applications but up to the present it has shown no indication of becoming routine

The vast majority of magnetic resonance work is based on high field conditions where eigenstates are pure Zeeman product states Inspection of the Figures 6 and 7 gives the impression that avoided crossing effects are very common, and that one might generally have to pay more attention to cross relaxation effects in conventional magnetic resonance of radicals This impression needs relativation

First, it is noteworthy that in high fields the electron spin α and the β manifolds are well separated in energy, and that they therefore do not cross For this reason, there can be direct additional contributions only to nuclear but not to electron relaxation For a discussion, Table 2 gives coupling constants for a number of common nuclei which give rise to avoided crossings near a field of 3300 Gauss as is often used in ESR or in ENDOR

Second, in low viscosity liquid solution one has isotropic conditions and only avoided crossings which obey the selection rule $\Delta M = 0$ We see from equation 8 that one needs nuclei with different magnetogyric ratios to produce such a transition The most common organic radicals contain only protons as magnetic nuclei so that the effect will not be encountered For different nuclei (one of them is assumed to be H here) the mixing rate between the two states induces a maximum nuclear relaxation at the crossing of $T_1^{-1} = \pi A^X_{iso} A^H_{iso} / B_r \gamma_e$ A relatively large effect is obtained for X = F for which T_1 becomes *ca* 1 μs

The situation is of much more concern in the case of static anisotropy or of slow reorientational dynamics The mixing rate at the maximum is orientation dependent, and for a nucleus X it is in the absence of dynamics given by $T_1^{-1} = 3\pi D^X_\perp \sin\theta \cos\theta$ For an anisotropy of 10 MHz one thus achieves relaxation times

Table 2 Interference of avoided level crossings in an ESR experiment at 3300 Gauss

X	$A^X_{iso}(\Delta M = 1)$ MHz	$\lvert A^H_{iso} - A^X_{iso}\rvert(\Delta M = 0)$ MHz
H	28 1	—
D	4 3	23 8
^{13}C	7 1	21 0
^{14}N	2 0	26 1
^{19}F	26 4	1 7
^{31}P	11 4	16 7
^{79}Br	7 0	21 1

of the order of 10 ns While this value relates directly to the two levels which are near-degenerate and thus to the ENDOR line at close to zero frequency which is not usually our focus, it is likely that in the complex relaxation scheme governing the ENDOR effect the high frequency line is also affected Furthermore, a recent study of the effect of dynamics shows that the onset of reorientational motion leads to an extreme broadening of the $\Delta M = 1$ resonance while their amplitude is only moderately affected For reorientational correlation times of the order of $(3\pi D_\perp)^{-1}$ one finds a nearly flat background relaxation, and it is only when motion becomes much faster that relaxation loses its importance [18]

The enormous sensitivity of the μSR technique may be demonstrated by the following fictitious example Suppose we are irradiating a sample with 10^5 muons per second, as in a typical time resolved experiment, and suppose we started to do this 10^{10} years ago, just after the Big Bang, and that we have never ceased to do so Let us assume further that the muons have a lifetime as long as the protons, and that they are thus still in the sample Today we would have accumulated some 3×10^{22} muons, which is one-twentieth of a mole, or 5 5 mg This is just to demonstrate that we have not reported on a new method for organic synthesis!

Acknowledgements Support from the Swiss National Foundation for Scientific Research and by the Paul Scherrer Institute in Villigen is gratefully acknowledged I am particularly indebted to my numerous co-workers and collaborators for their dedication and their practical and conceptual work The present work would have been impossible without their contributions

6 References

1 S F J Cox, *J Phys C Solid State Phys*, 1987, **20**, 3187
2 D C Walker, *J Phys Chem*, 1981, **85**, 3960
3 D C Walker, 'Muon and Muonium Chemistry', Cambridge University Press, 1983
4 E Roduner, 'The Positive Muon as a Probe in Free Radical Chemistry Potential and Limitations of the μSR Techniques', Lecture Notes in Chemistry, Vol 49, Springer, Heidelberg, 1988
5 T G Eck, L L Foldy, and H Wieder, *Phys Rev Lett*, 1973, **6**, 239
6 R F Haglund, *Chem Rev*, 1988, **88**, 697
7 S Clough, A J Horsewill, M R Johnson, M A Mohammed, T Newton, *Chem Phys*, 1991, **152**, 343
8 C A Hamilton, K A McLauchlan, and K R Peterson, *Chem Phys Lett* 1989, **162**, 145
9 *Chem Phys*, special issue, 1991, **152**, 229 337
10 A Carrington and A D McLachlan, 'Introduction to Magnetic Resonance' Harper, New York, 1967
11 E Roduner, R Crockett, and L M Wu, *J Chem Soc Faraday Trans*, 1993, **89**, 2101
12 E Roduner and H Fisher, *Chem Phys*, 1981, **54**, 261
13 N M Atherton, 'Electron Spin Resonance', Wiley, New York, 1973
14 M Heming, E Roduner, B D Patterson, W Odermatt, J W Schneider, H Baumeler, H Keller, and I M Savic, *Chem Phys Lett*, 1986, **128**, 100
15 R F Kiefl, *Hyperfine Int*, 1986, **32**, 707
16 E Roduner, I D Reid, M Ricco, and R De Renzi, *Ber Bunsenges Phys Chem*, 1989, **93**, 1194

17 M Heming, E Roduner, I D Reid, P W F Louwrier, J W Schneider, H Keller, W Odermatt, B D Patterson, H Simmler, B Pumpin, and I M Savic, *Chem Phys*, 1989, **129**, 335
18 S R Kreitzman and E Roduner, *Chem Phys*, to be submitted
19 E Roduner, *Chimia*, 1989, **43**, 86
20 R L Garwin, L M Ledermann, and M Weinrich, *Phys Rev*, 1957, **105**, 1415
21 E Roduner and I D Reid, *Israel J Chem*, 1989, **29**, 3
22 C J Rhodes, E Roduner, I D Reid, and T Azuma, *J Chem Soc, Chem Commun*, 1991, 208
23 U Haeberlen and G Maier, *Z Naturforsch A*, 1967, **22**, 1236
24 I D Reid and E Roduner, *Structural Chemistry*, 1991, **2**, 419
25 M Ricco, R De Renzi, and E Roduner, *Phys Lett A*, 1988, **129**, 390
26 Ch Niedermayer, I D Reid, E Roduner, E J Ansaldo, C Bernhard, U Binninger, J I Budnik, H Gluckler, E Recknagel, and A Weidinger, *Phys Rev B*, 1993, **47**, 10923
27 T J S Dennis, K Prassides, E Roduner, G Cristofolini, and R De Renzi, *J Phys Chem*, 1993, **97**, in press
28 K Prassides, T J S Dennis, C Christides, E Roduner, H W Kroto, R Taylor, and D R M Walton, *J Phys Chem*, 1992, **96**, 10600
29 I D Reid, T Azuma, and E Roduner, *Nature*, 1990, **345**, 328